

## Importance of Methane Chemical Potential for Its Conversion to Methanol on Cu-Exchanged Mordenite

Zheng, Jian; Lee, Insu; Khramenkova, Elena; Wang, Meng; Peng, Bo; Gutiérrez, Oliver Y.; Fulton, John L.; Camaioni, Donald M.; Pidko, Evgeny A.; More Authors

**DOI**

[10.1002/chem.202000772](https://doi.org/10.1002/chem.202000772)

**Publication date**

2020

**Document Version**

Final published version

**Published in**

Chemistry - A European Journal

**Citation (APA)**

Zheng, J., Lee, I., Khramenkova, E., Wang, M., Peng, B., Gutiérrez, O. Y., Fulton, J. L., Camaioni, D. M., Pidko, E. A., & More Authors (2020). Importance of Methane Chemical Potential for Its Conversion to Methanol on Cu-Exchanged Mordenite. *Chemistry - A European Journal*, 26(34), 7563-7567. <https://doi.org/10.1002/chem.202000772>

**Important note**

To cite this publication, please use the final published version (if applicable). Please check the document version above.

**Copyright**

Other than for strictly personal use, it is not permitted to download, forward or distribute the text or part of it, without the consent of the author(s) and/or copyright holder(s), unless the work is under an open content license such as Creative Commons.

**Takedown policy**

Please contact us and provide details if you believe this document breaches copyrights. We will remove access to the work immediately and investigate your claim.

## Heterogeneous Catalysis | Hot Paper |

## Importance of Methane Chemical Potential for Its Conversion to Methanol on Cu-Exchanged Mordenite

Jian Zheng,<sup>\*,[a]</sup> Insu Lee,<sup>[b]</sup> Elena Khramenkova,<sup>[c]</sup> Meng Wang,<sup>[a]</sup> Bo Peng,<sup>[a]</sup> Oliver Y. Gutiérrez,<sup>[a]</sup> John L. Fulton,<sup>[a]</sup> Donald M. Camaioni,<sup>[a]</sup> Rachit Khare,<sup>[b]</sup> Andreas Jentys,<sup>[b]</sup> Gary L. Haller,<sup>[d]</sup> Evgeny A. Pidko,<sup>[c]</sup> Maricruz Sanchez-Sanchez,<sup>\*,[b]</sup> and Johannes A. Lercher<sup>\*,[a, b]</sup>

**Abstract:** Copper-oxo clusters exchanged in zeolite mordenite are active in the stoichiometric conversion of methane to methanol at low temperatures. Here, we show an unprecedented methanol yield per Cu of 0.6, with a 90–95% selectivity, on a MOR solely containing  $[\text{Cu}_3(\mu\text{-O})_3]^{2+}$  active sites. DFT calculations, spectroscopic characterization and kinetic analysis show that increasing the chemical potential of methane enables the utilization of two  $\mu\text{-O}$  bridge oxygen out of the three available in the tricopper-oxo cluster structure. Methanol and methoxy groups are stabilized in parallel, leading to methanol desorption in the presence of water.

Selective oxidation of methane to methanol at low temperatures continues to pose a challenge. Because of the low reactivity of  $\text{CH}_4$  in comparison to the partial oxidation products the reaction tends to over-oxidation unless the oxidant is stoichiometrically limited. Enzymes such as particulate methane monooxygenases (pMMO) convert methane to methanol under aerobic conditions at Cu-centers.<sup>[1]</sup> Spectroscopic studies

indicate that the active sites in pMMO are Cu-oxo species containing 1–3 Cu atoms.<sup>[2]</sup> Inspired by this, Cu-oxo clusters immobilized in porous inorganic supports such as zeolites, silica, and metal-organic frameworks (MOFs) have been explored and show activity toward selectively converting methane to methanol at temperatures below 200 °C.<sup>[3]</sup>

On Cu-containing zeolites, methanol is synthesized stepwise, by sequentially dosing  $\text{O}_2$  and  $\text{CH}_4$ , followed by steam-assisted methanol desorption. This procedure leads to high selectivity to methanol, although requiring reconstitution of the active site after each cycle.<sup>[4]</sup> The yield of methanol offers direct information on the utilization of the oxygen at these active Cu sites.

Commonly, the molar ratio of formed methanol to Cu ions ( $\text{mol}_{\text{MeOH}}/\text{mol}_{\text{Cu}}$ ) is below 0.1.<sup>[5]</sup> Using an optimized preparation protocol, single site trinuclear copper-oxo clusters in mordenite (MOR) were synthesized and increased the yields to  $\approx 0.3 \text{ mol}_{\text{MeOH}}/\text{mol}_{\text{Cu}}$ .<sup>[6]</sup> More recently, Pappas et al. have reported a methanol yield of 0.47 in CuMOR and attributed it to the activity of  $[\text{Cu}_2(\mu\text{-O})]^{2+}$  sites.<sup>[7]</sup> This value of 0.47 is near the upper limit possible to achieve for an active  $[\text{Cu}_2(\mu\text{-O})]^{2+}$  site.

Increasing methane pressure has been reported to enhance the productivity and selectivity of methanol in continuous methane oxidation operation.<sup>[8]</sup> Tomkins et al. showed that a higher yield of methanol was achieved with CuMOR by increasing the methane pressure.<sup>[9]</sup> Brezicki et al. also observed that elevated  $\text{CH}_4$  pressure in the stepwise process promoted the conversion of  $\text{CH}_4$  on CuMOR, shifting the  $\text{MeOH}/\text{Cu}$  stoichiometry from 0.3 to 0.42.<sup>[10]</sup>

We have previously shown that trinuclear copper-oxo clusters  $[\text{Cu}_3(\mu\text{-O})_3]^{2+}$  are selectively formed, when preparing CuMOR by pH controlled ion exchange followed by activation in  $\text{O}_2$  at 500 °C.<sup>[6a]</sup> The yields of ca.  $0.3 \text{ mol}_{\text{MeOH}}/\text{mol}_{\text{Cu}}$  were, thus, attributed to the reaction of one  $\mu\text{-O}$  atom per  $[\text{Cu}_3(\mu\text{-O})_3]^{2+}$  cluster.<sup>[6a]</sup> Theory, however, had predicted that this cluster in MOR should be able to react consecutively with two  $\text{CH}_4$  molecules to produce stoichiometric amounts of  $\text{CH}_3\text{OH}$ .<sup>[11]</sup>

Here, we address the question, how substantially higher yields of methanol ( $0.6 \text{ mol}_{\text{MeOH}}/\text{mol}_{\text{Cu}}$ ) can be achieved when using single site CuMOR for the stoichiometric reaction with methane at 40 bar. For such CuMOR materials, the quantity of activated methane and the selectivity to methanol depend strongly on the reaction temperature and the methane pressure, as well as on the time that methane is in contact with

[a] Dr. J. Zheng, Dr. M. Wang, Dr. B. Peng, Dr. O. Y. Gutiérrez, J. L. Fulton, Dr. D. M. Camaioni, Prof. Dr. J. A. Lercher  
Institute for Integrated Catalysis, Pacific Northwest National Laboratory  
P.O. Box 999, Richland, WA 99352 (USA)  
E-mail: jian.zheng@pnnl.gov

[b] I. Lee, R. Khare, Dr. A. Jentys, Dr. M. Sanchez-Sanchez, Prof. Dr. J. A. Lercher  
Department of Chemistry and Catalysis Research Institute  
TU München, Lichtenbergstrasse 4, 85748 Garching (Germany)  
E-mail: m.sanchez@tum.de  
Johannes.Lercher@ch.tum.de

[c] E. Khramenkova, Prof. Dr. E. A. Pidko  
Inorganic Systems Engineering (ISE), Department of Chemical Engineering  
Delft University of Technology, 2629 HZ Delft (The Netherlands)

[d] Prof. Dr. G. L. Haller  
Department of Chemical and Environmental Engineering  
Yale University, New Haven, CT 06520 (USA)

Supporting information and the ORCID identification number(s) for the author(s) of this article can be found under:  
<https://doi.org/10.1002/chem.202000772>.

© 2020 The Authors. Published by Wiley-VCH Verlag GmbH & Co. KGaA. This is an open access article under the terms of Creative Commons Attribution NonCommercial-NoDerivs License, which permits use and distribution in any medium, provided the original work is properly cited, the use is non-commercial and no modifications or adaptations are made.

the sample (Figures 1, S11 and S12 for a CuMOR containing  $434 \mu\text{mol g}^{-1}$  of Cu). The example in Figure 1a shows the effect of the time that methane is in contact with CuMOR at a certain pressure on the yield of methanol. As the loading time increased from 15 to 180 minutes at 1 bar, the methanol yield increased from 0.11 to  $0.24 \text{ mol}_{\text{MeOH}}/\text{mol}_{\text{Cu}}$ ; that is, from  $47$  to  $100 \mu\text{mol g}^{-1}$ , including dimethyl ether (DME) counted as equivalent of 2 methanol molecules. Increasing the methane contact time further had only a minor impact. At 40 bar, approximately  $0.29 \text{ mol}_{\text{MeOH}}/\text{mol}_{\text{Cu}}$  ( $126 \mu\text{mol g}^{-1}$  of methanol) were produced already after 15 minutes. After 180 minutes, the methanol yield reached  $0.58 \text{ mol}_{\text{MeOH}}/\text{mol}_{\text{Cu}}$  ( $251 \mu\text{mol g}^{-1}$ ). Longer loading times did not increase the methanol yield. Figure 1b shows the dependence of the methanol yield on pressure (contact time: 180 minutes). The methanol yield normalized per Cu increased from 0.24 to  $0.58 \text{ mol}_{\text{MeOH}}/\text{mol}_{\text{Cu}}$  as the pressure increased from 1 to 40 bar. Increasing the methane pressure above 40 bar did not increase the methanol yield significantly. Control experiments by varying the amount of CuMOR showed that the amount of methanol formed increased linearly with the amount of CuMOR used. Thus, the methanol production normalized to the amount of Cu was constant at  $\approx 0.6 \text{ mol}_{\text{MeOH}}/\text{mol}_{\text{Cu}}$  (Figure 1c). Experiments using CuMOR with varying Cu contents (from pristine HMOR to  $461 \mu\text{mol g}^{-1}$  of Cu) showed that the amount of methanol produced at 40 bar also increased linearly with the Cu content of

MOR (Figure 1d). The correlation shows a methanol productivity of  $\approx 0.6 \text{ mol}_{\text{MeOH}}/\text{mol}_{\text{Cu}}$  for all Cu exchanged MOR, which suggests that there is mainly one type of active site in this series of CuMOR.

We also investigated the effect of catalyst activation temperature and methane loading temperature on the reaction. Activating CuMOR in oxygen at high temperature ( $\geq 500^\circ\text{C}$ ) was necessary to form a high concentration of active sites (Figure S12a). For the methane reaction step,  $200\text{--}220^\circ\text{C}$  was found to be the optimum temperature range (Figure S12b). At all reaction conditions tested here, we performed multiple three-stage reaction cycles to show the regenerability of the active sites of CuMOR. The methane loading time in the cycling tests was fixed to 180 min. Figure S11 shows that identical yields and selectivities were obtained in consecutive cycles over CuMOR both at 1 bar and 40 bar  $\text{CH}_4$  conditions. Even under the high reducing potential of 40 bar of  $\text{CH}_4$ , a constant methanol yield and product selectivity was obtained for up to 6 reaction cycles (Figure S15). This shows that active sites are fully regenerated during oxygen activation step and that the CuMOR materials studied here can be regarded as catalysts.

Since the results above showed that there is mainly one kind of active site, we focused on the CuMOR with  $434 \mu\text{mol g}^{-1}$  of Cu for spectroscopic analysis to gain insight into the nature and oxidation potential of the active Cu-oxo species. Let us first compare the product distribution at 1 and 40 bar of methane exposure (Figure S11). At 1 bar, the yields of methanol, DME, and  $\text{CO}_2$  were  $81$ ,  $9.5$ , and  $21 \mu\text{mol}/\text{g}_{\text{catalyst}}$  respectively. Taking into account that each molecule of  $\text{CO}_2$  is associated to the formation of 2  $\text{H}_2\text{O}$  molecules, this result indicates that the material has activated  $120 \mu\text{mol}/\text{g}_{\text{cat}}$  of  $\text{CH}_4$  and has introduced a total of  $184 \mu\text{mol}/\text{g}_{\text{cat}}$  ( $100$  plus  $21 \times 4$ ) of oxygen atoms to oxidation products. Assuming the absence of Cu spectators and only the existence of active  $[\text{Cu}_3(\mu\text{-O})_3]^{2+}$  clusters in this sample,<sup>[6a]</sup> the maximum concentration of trimers would be ca.  $145 \mu\text{mol}/\text{g}_{\text{cat}}$  ( $434/3$ ) and the concentration of potentially active  $\mu\text{-O}$  bridges is  $434 \mu\text{mol}/\text{g}_{\text{cat}}$ . This is consistent with oxidation of one  $\text{CH}_4$  by one  $\mu\text{-O}$  from the oxo cluster. When the reaction is performed at 40 bar, the productivity of methanol and  $\text{CO}_2$  was  $251$  and  $16 \mu\text{mol}/\text{g}_{\text{cat}}$ . This corresponds to a total  $267 \mu\text{mol}/\text{g}_{\text{cat}}$  of  $\text{CH}_4$  activated and a total amount of  $315 \mu\text{mol}/\text{g}_{\text{cat}}$  ( $251$  plus  $16 \times 4$ ) of O atoms. This corresponds to an average of two  $\text{CH}_4$  molecules activated and two  $\mu\text{-O}$  bridging atoms involved in oxidation processes in a trimeric Cu cluster. In light of this, we hypothesize that the higher chemical potential of methane at 40 bar allows utilization of two oxygen atoms per Cu-oxo cluster, and, thus, doubles of the productivity to methanol.

We have probed the state and constitution of active sites after reactions at low and high pressure of methane with magic-angle spinning nuclear magnetic resonance (MAS NMR) and in situ infrared (IR) spectroscopy. Typically, the NMR spectra were observed at  $25^\circ\text{C}$  after the catalyst had been reacted with methane or had methanol adsorbed at  $200^\circ\text{C}$ . The  $^{13}\text{C}$  NMR spectra (Figure S5) show that both methoxy species and adsorbed methanol are present after methane exposure. The  $^1\text{H}$  NMR spectra (Figure 2a) show two intense resonances

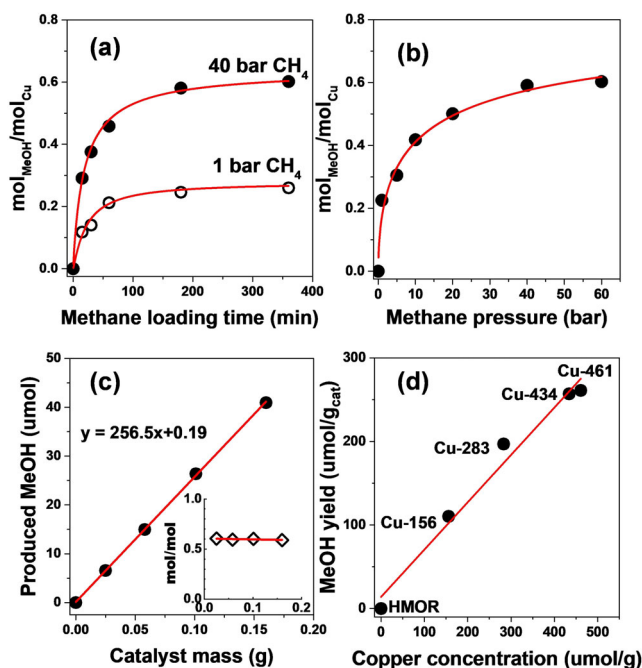


**Figure 1.** Methanol (MeOH) yield as a function of (a) methane loading time, (b) methane pressure, (c) amount of CuMOR (with a Cu content of  $434 \mu\text{mol g}^{-1}$ ) used at 40 bar  $\text{CH}_4$ , and (d) Cu concentration, for example, namely 0 (pristine HMOR), 156, 283, 434, and  $461 \mu\text{mol g}^{-1}$  used at 40 bar  $\text{CH}_4$ . The inset in (c) shows the molar ratio of produced MeOH to the amount of Cu in the materials. Typical reaction conditions: activation in 1 bar of  $\text{O}_2$  at  $500^\circ\text{C}$  for 2 h,  $\text{CH}_4$  exposure at  $200^\circ\text{C}$  for 3 h (except in (a)), and steam-assisted product extraction with 10 vol.% water steam in He at  $135^\circ\text{C}$  for 3 h.

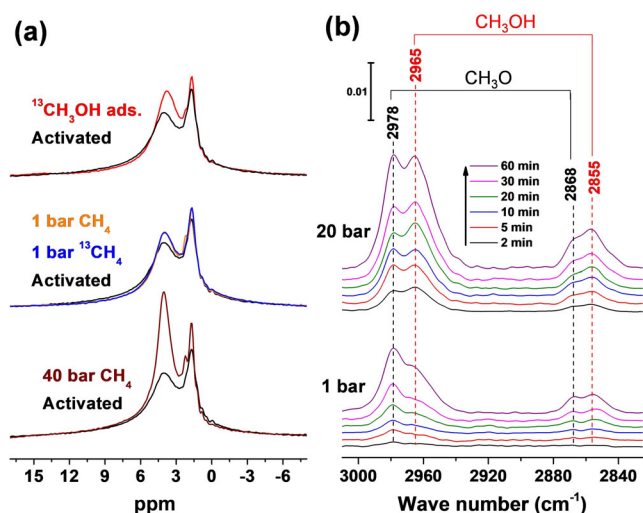


**Figure 2.** (a) Comparison of  $^1\text{H}$  cross-polarization (CP) MAS NMR spectra of a CuMOR (Cu concentration  $434 \mu\text{mol/g}_{\text{cat}}$ ) collected at room temperature after the treatment under different conditions:  $\text{O}_2$  activated at  $500^\circ\text{C}$  (black), unlabeled  $\text{CH}_4$  loaded at 1 bar (orange) and 40 bar (wine),  $^{13}\text{C}$ -labeled  $\text{CH}_4$  loaded at 1 bar (blue), and  $^{13}\text{C}$ -labeled  $\text{CH}_3\text{OH}$  adsorbed (red). (b) Time-resolved in situ FTIR spectra collected during the interaction of activated CuMOR (Cu concentration  $434 \mu\text{mol/g}_{\text{cat}}$ ) with 1 bar (bottom) and 20 bar (top) of methane at  $200^\circ\text{C}$ .

at 1.7 and 3.9 ppm that are assigned to  $\text{SiOH}$  and Brønsted acidic  $\text{Si}(\text{OH})\text{Al}$  groups, respectively.<sup>[12]</sup> Exposure to methanol led to a resonance at  $\approx 3.7$  ppm assigned to the hydrogens of methanol, which is difficult to differentiate from the protons of Brønsted acid sites.<sup>[13]</sup> Comparing the spectra of CuMOR acquired after exposure to 1 bar (blue and orange) and 40 bar (brown) methane, the peak at 3.9 ppm was more intense than at 1 bar (normalized to the intensity of the silanol peak) after methane loading at 40 bar. This increase in intensity is attributed to the presence of a larger concentration of methyl groups and/or additional  $\text{SiOHAl}$  groups formed by the reaction at high pressure. There is also a weak contribution at 2.2 ppm, which is tentatively attributed to hydroxyl groups bonded to the extra-framework aluminum.<sup>[14]</sup>

The NMR spectra agree well with in situ IR spectra recorded during the interaction of activated CuMOR with 1 and 20 bar of methane. Figure 2b shows bands at 2978, 2965 and 2868, 2858  $\text{cm}^{-1}$  corresponding to the asymmetric and symmetric vibrations of C–H in methyl groups of methoxy and methanol, respectively.<sup>[15]</sup> Consistent with these observations, control experiments showed that a fraction of methanol adsorbed on BAS in CuMOR reacted at  $200^\circ\text{C}$  to methoxy species and DME (Figures S6). We note that the intensities of these bands are significantly enhanced by increasing methane pressure. For example, contacting the CuMOR with 20 bar of methane for 5 minutes showed a similar band intensity to that of 1 bar for 60 minutes. The relative intensities indicate that a larger concentration of adsorbed methanol relative to methoxy species is formed at high pressures.

X-ray absorption spectroscopy (XAS) was used to assess the structure of Cu-oxo clusters and the changes they undergo upon reaction at different  $\text{CH}_4$  pressures. Figure S7 shows the

phase-uncorrected  $k^3$ -weighted  $\text{Mag}[x(\text{R})]$  and  $\text{Im}g[x(\text{R})]$  plots. All three samples show nearly the same average Cu–O distance. But the sample exposed to 1 bar  $\text{CH}_4$  has a lower amplitude, indicating a lower coordination number. The Cu–Cu path shows a signal at 2.3 Å, which shifts to higher values after methane exposure, especially at high pressure, compared with that of activated CuMOR. The amplitude of this feature decreased upon reaction with  $\text{CH}_4$ . Fitting the EXAFS spectra shows that the average Cu–Cu coordination number (CN) decreased from 2 in  $[\text{Cu}_3(\mu\text{-O})_3]^{2+[\text{6a}]}$  to  $1.1 \pm 0.8$  and  $0.6 \pm 0.4$  after the sample was exposed to 1 and 40 bar of methane (Figures S9, S10, Tables S2, S3). Including a Cu–C path for methanol or methoxy species slightly improved the fit quality and gave a Cu–C CN of 0.4–0.5 for both 1 and 40 bar experiments. The obtained Cu–C distance ( $\approx 3.05 \text{ \AA}$ ) was larger than the Cu–Cu distance ( $\approx 2.96 \text{ \AA}$ ) (Figures S9, S10, Tables S2, S3).

Combining the product yield data and spectroscopic observations, we propose that  $\text{CH}_4$  at 1 bar and  $200^\circ\text{C}$  reacts with one  $\mu\text{-O}$  bridge of the  $[\text{Cu}_3(\mu\text{-O})_3]^{2+}$ , forming methanol binding to the Cu site. Consequently, the Cu–Cu path becomes more disordered, which leads to a decrease in the Cu–Cu CN. At 40 bar, the stoichiometry of 0.6 MeOH per Cu in a sample with virtually no spectators can be explained by the reaction of  $\text{CH}_4$  with two  $\mu\text{-O}$  bridge atoms in the cluster. The conversion of two  $\text{CH}_4$  molecules leaves the active site in a highly disordered state and, thus, with a lower Cu–Cu CN.

It must be emphasized that, according to experiments in Figure 1 a, activation of  $\text{CH}_4$  by the first  $\mu\text{-O}$  site is very fast at 40 bar. This is shown by our kinetic analysis assuming a two-step reaction of methane with Cu-oxo clusters, where the rate constant for the oxidation of the first  $\text{CH}_4$  molecule is found to be two orders of magnitude larger than that of oxidation of a second molecule. For more details, see Supporting Information section “Kinetic analysis”. Thus, if a site with two active oxygen atoms is hypothesized, the first oxygen reacting rapidly with methane and the second oxygen reacting slower, both exhibit a reaction order of 1. Similarly, reaction of  $\text{CH}_4$  at 1 bar with the first  $\mu\text{-O}$  site also shows a reaction order of 1 in methane.

The thermodynamic limitations on the stoichiometry of methane oxidation by a model  $[\text{Cu}_3(\mu\text{-O})_3]^{2+}/\text{MOR}$  (Figure 3a) and their condition dependency were evaluated by an ab initio thermodynamic analysis (aiTA) based on periodic DFT calculations (see the Supporting Information for details). In line with previous experimental findings,<sup>[6a]</sup> the 8-MR of the MOR side pocket was selected as the preferred site for the stabilization of the trinuclear  $\text{Cu}_3\text{O}_3^{2+}$  cluster. Figure 3b presents the computed reaction Gibbs free energies ( $\Delta G$ ) for the sequential  $\text{CH}_4$  activation by  $[\text{Cu}_3(\mu\text{-O})_3]^{2+}/\text{MOR}$  as a function of the chemical potential of  $\text{CH}_4$ ,  $\Delta\mu_{\text{CH}_4}$ . The most stable  $\text{CH}_4$  oxidation intermediates are shown in Figure 3c. The results of the DFT and aiTA calculations show that under all practical  $T$  and  $p_{\text{CH}_4}$  as represented by the relevant range of  $\Delta\mu_{\text{CH}_4}$ , the stoichiometry for  $\text{CH}_4$  activation by  $[\text{Cu}_3(\mu\text{-O})_3]^{2+}$  is limited to 2  $\text{CH}_4$  per 3 Cu. While the activation of the first  $\text{CH}_4$  ( $1\text{CH}_4 \cdot \text{Cu}_3\text{O}_3$ ) is strongly exergonic at all  $\Delta\mu_{\text{CH}_4}$ , elevated  $p_{\text{CH}_4}$  is required for favorable thermodynamics to oxidize a second  $\text{CH}_4$  molecule by the copper trimer ( $2\text{CH}_4 \cdot \text{Cu}_3\text{O}_3$ , Figure 3b).

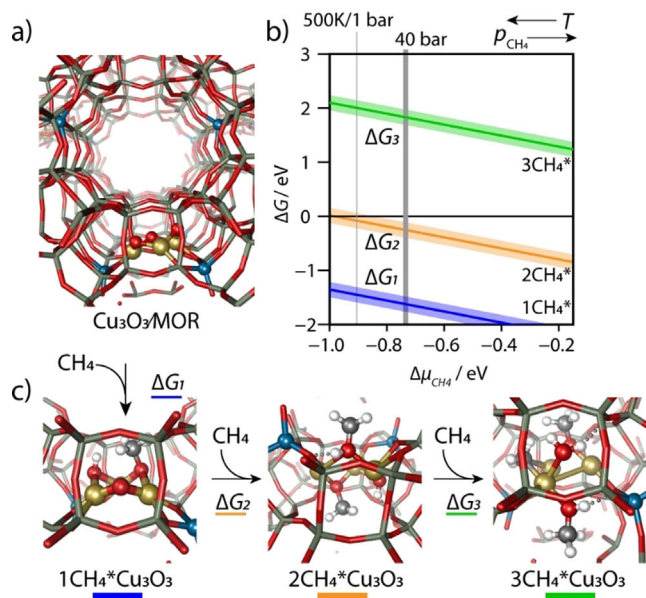


**Figure 3.** (a) The structure of the active Cu<sub>3</sub>O<sub>3</sub>/MOR site sitting in the MOR side pocket, (b) the computed Gibbs free energies of sequential methane activation by this cluster as a function of  $\Delta\mu_{\text{CH}_4}$  and (c) the local optimized geometries of the corresponding surface products.

Similar conclusions are obtained, if calculations are performed for the Cu<sub>3</sub>O<sub>3</sub> cluster in the 12-MR channel, an alternative position of the Cu<sub>3</sub>O<sub>3</sub> cluster (Figure S18). Importantly, the stable intermediates of two CH<sub>4</sub> oxidation feature a partially reduced Cu cluster with CH<sub>3</sub>OH and CH<sub>3</sub>O<sup>-</sup> ligands capable of producing methanol during the post-reaction steaming treatment. The activation of a third CH<sub>4</sub> molecule yields an intermediate with a Cu–CH<sub>3</sub> moiety, which would produce methane upon reaction with H<sub>2</sub>O. The formation of such an intermediate has been found to be unfavorable even at pressures much greater than 40 bar.<sup>[16]</sup>

In summary, we present here evidence for an unprecedented methanol yield per Cu in the low-temperature selective oxidation of methane with [Cu<sub>3</sub>(μ-O)<sub>3</sub>]<sup>2+</sup> clusters exchanged in MOR. The results indicate, however, that this stoichiometry of 0.6 mol<sub>MeOH</sub>/mol<sub>Cu</sub> is near the upper limit in this catalyst. Combined evaluation of the reactivity, spectroscopic studies, kinetics analysis, and DFT calculations showed that methanol yields in CuMOR are maximized by increasing the chemical potential of methane to values enabling the activation of two CH<sub>4</sub> molecules at one active center containing three oxygen atoms.

## Acknowledgements

This research was supported by the U.S. Department of Energy (DOE), Office of Science, Office of Basic Energy Sciences (BES), Division of Chemical Sciences, Geosciences and Biosciences (Transdisciplinary Approaches to Realize Novel Catalytic Pathways to Energy Carriers, FWP 47319). In addition, J.Z. and O.Y.G. acknowledge support by the Inorganometallic Catalyst Design Center, an Energy Frontier Research Center funded by

the U.S. Department of Energy, Office of Science, Basic Energy Sciences under Award #DE-SC0012702. I.L. and M.S.S. are thankful to the Deutsche Forschungsgemeinschaft (DFG) and the TUM International Graduate School of Science and Engineering (IGSSE) for financial support. E.K. and E.A.P. acknowledge SurfSARA and NWO (The Netherlands Organisation for Scientific Research) for providing access to supercomputer resources and the European Research Council (ERC) for funding under the European Union's Horizon 2020 research and innovation programme (Grant Agreement No. 725686). We acknowledge the APS (Sector 20, supported by the U.S. Department of Energy, DE-AC02-06CH11357) and DESY (Hamburg, Germany), a member of the Helmholtz Association HGF, for the provision of experimental facilities for X-ray experiments.

## Conflict of interest

The authors declare no conflict of interest.

**Keywords:** chemical potential · copper-trimer · methane oxidation · methanol production · zeolite

- [1] S. I. Chan, S. S. F. Yu, *Acc. Chem. Res.* **2008**, *41*, 969–979.
- [2] V. C. C. Wang, S. Maji, P. R. Y. Chen, H. K. Lee, S. S. F. Yu, S. I. Chan, *Chem. Rev.* **2017**, *117*, 8574–8621.
- [3] a) C. C. Liu, C. Y. Mou, S. S. F. Yu, S. I. Chan, *Energ Environ Sci* **2016**, *9*, 1361–1374; b) J. Zheng, J. Ye, M. A. Ortuño, J. L. Fulton, O. Y. Gutiérrez, D. M. Camaioni, R. K. Motkuri, Z. Li, T. E. Webber, B. L. Mehdi, N. D. Browning, R. L. Penn, O. K. Farha, J. T. Hupp, D. G. Truhlar, C. J. Cramer, J. A. Lercher, *J. Am. Chem. Soc.* **2019**, *141*, 9292–9304; c) S. Grundner, W. Luo, M. Sanchez-Sanchez, J. A. Lercher, *Chem. Commun.* **2016**, *52*, 2553–2556; d) T. Ikuno, J. Zheng, A. Vjunov, M. Sanchez-Sanchez, M. A. Ortuno, D. R. Pahls, J. L. Fulton, D. M. Camaioni, Z. Y. Li, D. Ray, B. L. Mehdi, N. D. Browning, O. K. Farha, J. T. Hupp, C. J. Cramer, L. Gagliardi, J. A. Lercher, *J. Am. Chem. Soc.* **2017**, *139*, 10294–10301.
- [4] T. Ikuno, S. Grundner, A. Jentys, G. Li, E. A. Pidko, J. L. Fulton, M. Sanchez-Sanchez, J. A. Lercher, *J. Phys. Chem. C* **2019**, *123*, 8759.
- [5] a) J. S. Woertink, P. J. Smeets, M. H. Groothaert, M. A. Vance, B. F. Sels, R. A. Schoonheydt, E. I. Solomon, *Proc. Natl. Acad. Sci. USA* **2009**, *106*, 18908–18913; b) E. M. Alayon, M. Nachtegaal, M. Ranocchiari, J. A. van Bokhoven, *Chem. Commun.* **2012**, *48*, 404–406.
- [6] a) S. Grundner, M. A. Markovits, G. Li, M. Tromp, E. A. Pidko, E. J. Hensen, A. Jentys, M. Sanchez-Sanchez, J. A. Lercher, *Nat. Commun.* **2015**, *6*, 7546; b) Y. Kim, T. Y. Kim, H. Lee, J. Yi, *Chem. Commun.* **2017**, *53*, 4116–4119.
- [7] D. K. Pappas, A. Martini, M. Dyballa, K. Kvande, S. Teketel, K. A. Lomachenko, R. Baran, P. Glatzel, B. Arstad, G. Berlier, C. Lamberti, S. Bordiga, U. Olsbye, S. Svelle, P. Beato, E. Borfecchia, *J. Am. Chem. Soc.* **2018**, *140*, 15270–15278.
- [8] a) J. W. Chun, R. G. Anthony, *Ind. Eng. Chem. Res.* **1993**, *32*, 788–795; b) Q. H. Liu, J. Rogut, B. S. Chen, J. L. Falconer, R. D. Noble, *Fuel* **1996**, *75*, 1748–1754.
- [9] P. Tomkins, A. Mansouri, S. E. Bozbag, F. Krumeich, M. B. Park, E. M. C. Alayon, M. Ranocchiari, J. A. van Bokhoven, *Angew. Chem. Int. Ed.* **2016**, *55*, 5467–5471; *Angew. Chem.* **2016**, *128*, 5557–5561.
- [10] G. Brezicki, J. D. Kammert, T. B. Gunnoe, C. Paolucci, R. J. Davis, *ACS Catal.* **2019**, *9*, 5308–5319.
- [11] a) M. H. Mahyuddin, T. Tanaka, Y. Shiota, A. Staykov, K. Yoshizawa, *ACS Catal.* **2018**, *8*, 1500–1509; b) M. H. Mahyuddin, T. Tanaka, A. Staykov, Y. Shiota, K. Yoshizawa, *Inorg. Chem.* **2018**, *57*, 10146–10152.
- [12] G. Paul, C. Bisio, I. Braschi, M. Cossi, G. Gatti, E. Gianotti, L. Marchese, *Chem. Soc. Rev.* **2018**, *47*, 5684–5739.
- [13] Z. M. Yan, D. Ma, J. Q. Zhuang, X. C. Liu, X. M. Liu, X. W. Han, X. H. Bao, *Phys. Chem. Chem. Phys.* **2002**, *4*, 4602–4607.

- [14] J. Q. Zhuang, M. Ding, Y. Gang, Z. M. Yan, X. M. Liu, X. C. Liu, X. W. Han, X. H. Bao, X. Peng, Z. M. Liu, *J. Catal.* **2004**, 228, 234–242.
- [15] a) V. L. Sushkevich, D. Palagin, M. Ranocchiari, J. A. van Bokhoven, *Science* **2017**, 356, 523–527; b) G. Mirth, J. A. Lercher, M. W. Anderson, J. Klinowski, *J. Chem. Soc. Faraday T* **1990**, 86, 3039–3044.

- [16] G. Ferraudi, *Inorg. Chem.* **1978**, 17, 2506–2508.

---


Manuscript received: February 12, 2020

Accepted manuscript online: February 24, 2020



Version of record online: ■ ■ ■ ■ 0000

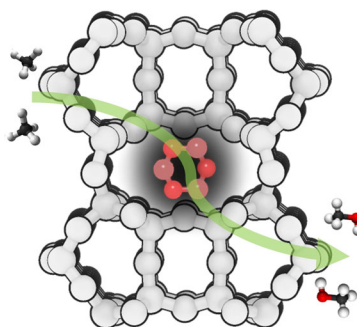
## COMMUNICATION

### Heterogeneous Catalysis

 J. Zheng,\* I. Lee, E. Khramenkova,  
M. Wang, B. Peng, O. Y. Gutiérrez,  
J. L. Fulton, D. M. Camaioni, R. Khare,  
A. Jentys, G. L. Haller, E. A. Pidko,  
M. Sanchez-Sanchez,\* J. A. Lercher\*



  **Importance of Methane Chemical  
Potential for Its Conversion to  
Methanol on Cu-Exchanged Mordenite**



**On the oxidation of methane:** Elevated methane pressure increased the chemical potential of methane to enable the activation of two CH<sub>4</sub> molecules by two  $\mu$ -O atoms out of the three contained in a [Cu<sub>3</sub>( $\mu$ -O)<sub>3</sub>]<sup>2+</sup> tricopper-oxo cluster.